

A LIGHTWEIGHT FOURIER-BASED NETWORK FOR BINAURAL SPEECH ENHANCEMENT WITH SPATIAL CUE PRESERVATION

Xikun Lu¹ Yujian Ma¹ Xianquan Jiang² Xuelong Wang³ Jinqiu Sang^{3*}

¹ Shanghai Institute of Artificial Intelligence for Education, East China Normal University, China

² Boin Hearing Technology (Shanghai) Co., LTD, China

³ School of Computer Science and Technology, East China Normal University, China

ABSTRACT

Binaural speech enhancement faces a severe trade-off challenge, where state-of-the-art performance is achieved by computationally intensive architectures, while lightweight solutions often come at the cost of significant performance degradation. To bridge this gap, we propose the Global Adaptive Fourier Network (GAF-Net), a lightweight deep complex network that aims to establish a balance between performance and computational efficiency. The GAF-Net architecture consists of three components. First, a dual-feature encoder combining short-time Fourier transform and gammatone features enhances the robustness of acoustic representation. Second, a channel-independent globally adaptive Fourier modulator efficiently captures long-term temporal dependencies while preserving the spatial cues. Finally, a dynamic gating mechanism is implemented to reduce processing artifacts. Experimental results show that GAF-Net achieves competitive performance, particularly in terms of binaural cues (ILD and IPD error) and objective intelligibility (MBSTOI), with fewer parameters and computational cost. These results confirm that GAF-Net provides a feasible way to achieve high-fidelity binaural processing on resource-constrained devices.

Index Terms— Binaural speech enhancement, complex neural network, lightweight model, Fourier network.

1. INTRODUCTION

Speech enhancement (SE) aims to improve speech quality and intelligibility by reducing background noise [1, 2]. However, for binaural listening devices such as hearing aids, it is essential to enhance speech clarity and preserve the spatial perception encoded by binaural cues [3]. While single-channel SE methods excel at noise reduction, their inherent design destroys the critical inter-channel relationships that constitute spatial cues [4, 5], making them unsuitable for binaural scenarios. This work focuses on binaural speech enhancement (BSE) to jointly optimize noise suppression and preserve binaural cues.

Statistical signal processing methods are initially applied to BSE tasks, such as the minimum variance distortionless response beamformer [6, 7] and the multichannel Wiener filter [8, 9, 10]. These methods perform well and efficiently under stationary acoustic conditions, but their performance degrades significantly in real-world non-stationary noisy environments. To overcome these limitations, studies have shifted towards deep-learning-based methods, particularly those performing end-to-end modeling in the complex do-

main [11, 12], which can generate higher-fidelity speech by jointly optimizing amplitude and phase.

Various deep learning strategies have emerged in the BSE field. Some studies attempt to maximize the signal-to-noise ratio (SNR) by processing binaural channels independently [13], at the expense of spatial fidelity. Other studies introduce complex-valued networks, but their design choices hinder the ability to fully exploit the advantages of complex-domain processing [14]. The demand for higher performance has led to the emergence of more sophisticated architectures, including parallel networks [15, 5] and complex Transformers [16], with the latter achieving state-of-the-art results. However, their large model size and computational overhead pose significant deployment barriers. To address this, efficient models have been proposed [17], which reduce complexity by selectively processing low-frequency components.

Despite these advances, existing methods still face several key limitations. First, the prevalent reliance on single short-time Fourier transform (STFT) features, of which the inherent trade-off between time and frequency resolution limits the model's acoustic representation capabilities. Second, a fundamental trade-off exists in effectively modeling long-range temporal dependencies: high-performance architectures like Transformers are computationally prohibitive, while lightweight alternatives often lack sufficient receptive field.

To address these challenges, this paper introduces the Global Adaptive Fourier Network (GAF-Net), a novel lightweight complex-valued network designed to achieve a balance among performance and efficiency. The effectiveness of our approach stems from three architectural innovations. First, We propose a dual-feature encoding and fusion module that simultaneously processes STFT-based features and psychoacoustically inspired features to form more robust input representations. Second, we introduce a lightweight Global Adaptive Fourier Modulator (GAFM) as the network backbone, which efficiently models global temporal dynamics in the Fourier domain while maintaining inter-channel independence to preserve spatial cues. Finally, we employ a soft-boundary dynamic gating mechanism to suppress processing artifacts and enhance perceptual naturalness by dynamically blending enhanced and original spectrograms.

2. PROPOSED METHOD

The objective of BSE is to recover clean speech signals $s_i(t)$ from noisy mixtures $y_i(t) = s_i(t) + n_i(t)$, where $i \in \{L, R\}$, while preserving spatial cues. This task is typically addressed in the time-frequency (T-F) domain, where the relationship is $\mathbf{Y}_i = \mathbf{S}_i + \mathbf{N}_i$. We propose a deep complex network, \mathcal{G} , that

* Corresponding author: jqsang@mail.ecnu.edu.cn

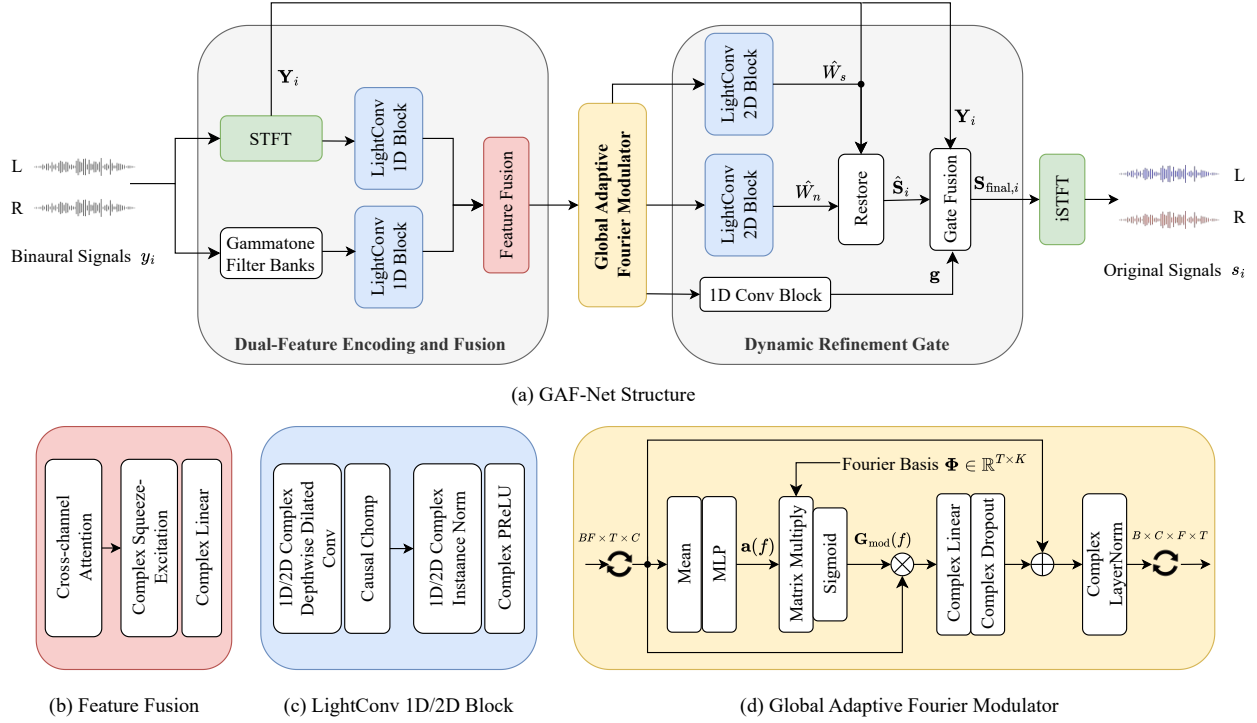


Fig. 1. The proposed GAF-Net model, which mainly consists of dual-feature encoding and fusion, global adaptive Fourier modulator, and dynamic refinement gate. Different modules are marked with different colors.

learns a direct mapping from the noisy to the estimated clean spectrograms: $\mathcal{G} : (\mathbf{Y}_L, \mathbf{Y}_R) \rightarrow (\mathbf{S}_L, \mathbf{S}_R)$. As depicted in Fig. 1, our model employs an encoder-decoder architecture featuring three core components: a dual-feature encoding and fusion module, a GAFM backbone, and a Dynamic Refinement Gate (DRG).

2.1. Dual-Feature Encoding and Fusion

To construct a comprehensive acoustic representation, a dual-stream encoder architecture is employed. The primary path generates standard complex STFT spectrograms, whereas the secondary path utilizes a gammatone filterbank to produce a perceptually-motivated representation. The spectrogram features from each path are first processed by separate encoders consisting of M layers of LightConv 1D blocks to extract high-level representations, denoted as \mathbf{Z}_{stft} and $\mathbf{Z}_{\text{gamma}}$, respectively. These representations are then fused using a cross-channel attention mechanism. Specifically, the magnitude of the gammatone features is used to generate an attention map that modulates the STFT feature path:

$$\mathbf{Z}_{\text{attended}} = \mathbf{Z}_{\text{stft}} \odot \sigma(\text{Conv}(|\mathbf{Z}_{\text{gamma}}|)) \quad (1)$$

where $\sigma(\cdot)$ is the sigmoid function. The fused features are further channel-wise recalibrated through a complex Squeeze-and-Excitation (SE) block to generate an overall representation for the backbone network.

2.2. Global Adaptive Fourier Modulator

We propose the GAFM as the backbone of our model to efficiently model long-range temporal dependencies. Unlike self-attention

mechanisms, which require quadratic complexity, GAFM integrates information by dynamically synthesizing a global filter for each input sequence.

Let the input to a GAFM block be the complex latent feature $\mathbf{Z}_{\text{bb}} \in \mathbb{C}^{B \times C \times F \times T}$. For each frequency-specific slice \mathbf{Z}_f , the module first extracts a compact global context vector $\mathbf{c}_f = \mathbb{E}_T[|\mathbf{Z}_f|]$ by averaging the feature magnitudes along the temporal dimension. This context vector is then fed into a small multilayer perceptron (MLP) to generate a set of mixing coefficients $\mathbf{a}(f) = \text{MLP}(\mathbf{c}_f) \in \mathbb{R}^K$. These coefficients are then used to form a linear combination of a fixed, predefined Fourier basis matrix $\Phi \in \mathbb{R}^{T \times K}$, thereby synthesizing a content-adaptive gating signal $\mathbf{G}_{\text{mod}}(f)$:

$$\mathbf{G}_{\text{mod}}(f) = \sigma(\tau \cdot \Phi \cdot \mathbf{a}(f)) \quad (2)$$

where $\sigma(\cdot)$ is the sigmoid function. Note that since the synthesis gate $\mathbf{G}_{\text{mod}}(f)$ is a real-valued gate, its element-wise multiplication with the original input \mathbf{Z}_f only modulates the magnitude of the complex features while strictly preserving their phase. This phase-preserving property is crucial for maintaining the Interaural Time Difference (ITD), a key cue for spatial localization [18]. Finally, the modulated features are integrated into a standard residual block:

$$\mathbf{Z}_{\text{out},f} = \text{CLN}(\mathbf{Z}_f + \text{CDropout}(\text{CLinear}(\mathbf{Z}_f \odot \mathbf{G}_{\text{mod}}))) \quad (3)$$

where CLinear denotes a complex linear layer, CLN denotes complex layer normalization, and dropout is applied in a way that preserves the complex structure. By performing these operations in parallel across all frequencies, GAFM efficiently models the global temporal context while ensuring the integrity of spatial information.

2.3. Binaural Decoding and Dynamic Refinement Gate

The decoder stage reconstructs the enhanced binaural signals from the backbone’s output features \mathbf{Z}_{out} . To this end, two parallel decoder heads are used to estimate Relative Acoustic Transfer Functions (RATFs) [19, 20]. The target speech RATF is denoted as $\hat{\mathbf{W}}_s$, and the noise RATF is denoted as $\hat{\mathbf{W}}_n$. The decoder head consists of N layers of LightConv 2D blocks.

Given the noisy observations and the estimated RATFs, the clean speech spectrograms $\hat{\mathbf{S}}_i$ can be recovered using the following closed-form solution:

$$\hat{\mathbf{S}}_L = \hat{\mathbf{W}}_s \cdot \hat{\mathbf{S}}_R, \quad \hat{\mathbf{S}}_R = \frac{(\mathbf{Y}_L - \hat{\mathbf{W}}_n \mathbf{Y}_R)(\hat{\mathbf{W}}_s - \hat{\mathbf{W}}_n)^*}{(\hat{\mathbf{W}}_s - \hat{\mathbf{W}}_n)^2 + \epsilon} \quad (4)$$

where ϵ is a small constant for numerical stability. To suppress potential processing artifacts and enhance model robustness, we introduce the DRG. This module generates a frequency-dependent gate $\mathbf{g} \in [0, 1]^{B \times F}$, which can be understood as a confidence map of the model’s enhancement result at each frequency. The gate is derived from the temporal aggregation information of the backbone features:

$$\mathbf{g} = \sigma(\text{Conv}_{1 \times 1}((\text{AvgPool}_T(|\mathbf{Z}_{\text{out}}|))) \quad (5)$$

The final output $\mathbf{S}_{\text{final}}$ is obtained by weighted summation of the network-estimated clean spectrogram $\hat{\mathbf{S}}$ and the original noisy spectrogram \mathbf{Y} , controlled by \mathbf{g} :

$$\mathbf{S}_{\text{final},i} = \mathbf{g} \odot \hat{\mathbf{S}}_i + (1 - \mathbf{g}) \odot \mathbf{Y}_i \quad (6)$$

This mechanism enables the model to trust its enhancement in high-confidence frequency regions ($\mathbf{g} \rightarrow 1$) while restoring to the original signal in the low-confidence areas ($\mathbf{g} \rightarrow 0$), thereby achieving a dynamic balance between denoising and fidelity. The refined binaural complex spectrogram is then transformed back to the time domain via the inverse STFT (iSTFT).

2.4. Loss Function

The proposed network is trained by optimizing a composite loss function $\mathcal{L}_{\text{total}}$, which consists of a primary task-oriented loss $\mathcal{L}_{\text{task}}$, and an regularization term \mathcal{L}_{reg} :

$$\mathcal{L}_{\text{total}} = \mathcal{L}_{\text{task}} + \mathcal{L}_{\text{reg}} \quad (7)$$

The primary task loss function $\mathcal{L}_{\text{task}}$ follows the design in [16] and is a weighted sum of four objectives, aiming to synergistically optimize denoising performance, speech intelligibility, and the preservation of binaural cues:

$$\mathcal{L}_{\text{task}} = \alpha \mathcal{L}_{\text{SNR}} + \beta \mathcal{L}_{\text{STOI}} + \gamma \mathcal{L}_{\text{ILD}} + \kappa \mathcal{L}_{\text{IPD}} \quad (8)$$

The time-domain terms \mathcal{L}_{SNR} and $\mathcal{L}_{\text{STOI}}$ represent noise suppression and intelligibility. The time-frequency terms, \mathcal{L}_{ILD} and \mathcal{L}_{IPD} , ensure accurate reconstruction of spatial information by penalizing the mean absolute error between the Interaural Level Difference (ILD) and Interaural Phase Difference (IPD) of the clean and enhanced signals.

The regularization term \mathcal{L}_{reg} is applied to the gating signal \mathbf{g} of the DRG to provide fine-grained control over its behavior. It consists of three parts:

$$\mathcal{L}_{\text{reg}} = \lambda_s \mathcal{R}_{\text{sparse}}(\mathbf{g}) + \lambda_e \mathcal{R}_{\text{entropy}}(\mathbf{g}) + \lambda_{tv} \mathcal{R}_{\text{TV}}(\mathbf{g}) \quad (9)$$

The three parts are: 1) an L1 sparse regularizer ($\mathcal{R}_{\text{sparse}}$) to promote conservative augmentation strategy; 2) a negative entropy regularizer ($\mathcal{R}_{\text{entropy}}$) to encourage decisive, binary-like gating decisions; and 3) a Total Variation (TV) regularizer (\mathcal{R}_{TV}) to enforce spectral smoothness.

3. EXPERIMENTS

3.1. Datasets

We construct a binaural speech dataset for training and testing our model. Clean monaural speech signals are sourced from the VCTK corpus [21], from which we generate 40,000 training, 5,000 validation, and 5,000 test samples, each with a duration of 2 seconds. To ensure a robust evaluation of generalization, a strict partitioning of data resources is enforced. Both the speakers from the VCTK corpus and the Head-Related Impulse Responses (HRIRs) from the HUTUBS database [22] are split into training, validation, and test-exclusive subsets. This speaker- and HRIR-disjoint strategy guarantees that the model encounters neither familiar speakers nor familiar acoustic transfer functions during validation and testing. During data synthesis, each monaural speech utterance is spatialized into a binaural signal by convolving it with a pair of HRIRs randomly selected from the corresponding subset. The target speech source is placed at a random azimuth in the horizontal plane, from -90° to $+90^\circ$. Noise signals are drawn from the NOISEX-92 database [23] and are synthesized into a diffuse isotropic noise field by convolving non-overlapping segments of a noise source with all available HRIRs on the horizontal plane for a given subject and summing the results. For the training and validation sets, noisy mixtures are generated at a random SNR continuously drawn from -7 dB to 16 dB. For the test set, fixed SNR levels ranging from -6 dB to 15 dB in 3 dB steps are used to facilitate a balanced performance assessment. The noise types used for training include white, pink, factory, and babble noise. During evaluation, an additional unseen noise type (car engine noise) is introduced to assess the model’s noise generalization capability. All audio data are generated at a sampling rate of 16 kHz.

3.2. Implementation Details

All audio signals are processed at a sampling rate of 16 kHz. For feature extraction, we employ an STFT with a 256-point FFT and a 128-sample hop size. The parallel Gammatone filterbank is configured with 64 channels. The model’s encoder consists of two layers of LightConv 1D blocks ($M = 2$), the backbone network is one layer of GAFM, and the decoder is two layers of LightConv 2D blocks ($N = 2$). For training, the AdamW optimizer is used with an initial learning rate of 2×10^{-4} . The model is trained for 100 epochs with a batch size of 20, using a multi-step learning rate scheduler. Early stopping is enabled to terminate training if the validation loss does not improve for 8 consecutive epochs. The weighting coefficients α, β, γ , and κ for the composite loss function are set to 1, 10, 1, and 10, respectively. The regularization weight λ_s, λ_e , and λ_{tv} are all set to 1×10^{-4} .

3.3. Evaluation Metrics

To comprehensively evaluate model performance, four standard objective metrics are employed. The gain of perceptual evaluation of speech quality (ΔPESQ) [24] quantifies the model’s perceptual quality improvement relative to the noisy input. The ILD error (\mathcal{L}_{ILD}) [16] and IPD error (\mathcal{L}_{IPD}) [16] are used to measure the reconstruction accuracy of spatial cues such as sound source localization. Finally, the Binaural Short-Time Objective Intelligibility (MB-STOI) [25] serves as a comprehensive metric that jointly assesses speech intelligibility and the integrity of binaural cues.

Table 1. Objective evaluation results under different input SNR conditions. The best results are marked in **bold**.

Input SNR	-6 dB				-3 dB				0 dB			
Method	MBSTOI \uparrow	Δ PESQ \uparrow	\mathcal{L}_{ILD} \downarrow	\mathcal{L}_{IPD} \downarrow	MBSTOI \uparrow	Δ PESQ \uparrow	\mathcal{L}_{ILD} \downarrow	\mathcal{L}_{IPD} \downarrow	MBSTOI \uparrow	Δ PESQ \uparrow	\mathcal{L}_{ILD} \downarrow	\mathcal{L}_{IPD} \downarrow
DBSEnh [14]	0.63	0.04	7.36	1.16	0.67	0.04	7.34	1.11	0.75	0.05	6.69	1.01
BiTasNet [15]	0.69	0.02	4.17	1.26	0.73	0.04	3.98	1.16	0.75	0.03	3.96	1.14
BCCTN [16]	0.71	0.08	5.91	1.08	0.78	0.14	5.60	1.02	0.80	0.25	4.89	0.86
LBCCN [17]	0.73	0.14	7.14	1.11	0.80	0.16	6.05	1.01	0.81	0.13	6.52	1.00
GAF-Net	0.77	0.09	5.23	0.99	0.80	0.14	4.89	1.02	0.84	0.19	4.62	0.89
Input SNR	3 dB				6 dB				9 dB			
Method	MBSTOI \uparrow	Δ PESQ \uparrow	\mathcal{L}_{ILD} \downarrow	\mathcal{L}_{IPD} \downarrow	MBSTOI \uparrow	Δ PESQ \uparrow	\mathcal{L}_{ILD} \downarrow	\mathcal{L}_{IPD} \downarrow	MBSTOI \uparrow	Δ PESQ \uparrow	\mathcal{L}_{ILD} \downarrow	\mathcal{L}_{IPD} \downarrow
DBSEnh [14]	0.80	0.05	6.41	1.00	0.84	0.10	5.94	0.89	0.84	0.12	5.56	0.83
BiTasNet [15]	0.78	0.08	3.82	1.18	0.81	0.11	3.80	1.12	0.78	0.10	3.67	1.13
BCCTN [16]	0.84	0.32	4.40	0.76	0.86	0.46	4.13	0.67	0.91	0.62	3.70	0.57
LBCCN [17]	0.85	0.23	5.80	0.96	0.88	0.27	4.73	0.86	0.87	0.25	4.62	0.84
GAF-Net	0.85	0.27	3.79	0.82	0.88	0.26	3.46	0.71	0.88	0.24	3.32	0.66
Input SNR	12 dB				15 dB				Average			
Method	MBSTOI \uparrow	Δ PESQ \uparrow	\mathcal{L}_{ILD} \downarrow	\mathcal{L}_{IPD} \downarrow	MBSTOI \uparrow	Δ PESQ \uparrow	\mathcal{L}_{ILD} \downarrow	\mathcal{L}_{IPD} \downarrow	MBSTOI \uparrow	Δ PESQ \uparrow	\mathcal{L}_{ILD} \downarrow	\mathcal{L}_{IPD} \downarrow
DBSEnh [14]	0.87	0.07	5.38	0.80	0.89	0.08	4.79	0.71	0.78	0.06	6.18	0.93
BiTasNet [15]	0.82	0.30	3.74	1.10	0.82	0.52	3.69	1.10	0.77	0.13	3.86	1.17
BCCTN [16]	0.92	0.60	3.63	0.56	0.90	0.58	3.35	0.50	0.84	0.35	4.59	0.79
LBCCN [17]	0.89	0.24	4.35	0.78	0.92	0.30	3.83	0.72	0.85	0.20	5.32	0.88
GAF-Net	0.89	0.27	3.00	0.50	0.94	0.27	2.53	0.44	0.86	0.22	3.86	0.75

Table 2. Parameter count and computational complexity.

Method	# Param. \downarrow	MACs \downarrow	RTF \downarrow
DBSEnh	10.5 M	0.99 G	0.026
BiTasNet	1.7 M	4.97 G	0.148
BCCTN	11.1 M	16.38 G	0.237
LBCCN	38.0 K	0.30 G	0.092
GAF-Net	129.0 K	2.79 G	0.150

Table 3. Ablation study of the proposed model components.

Method	MBSTOI \uparrow	Δ PESQ \uparrow	\mathcal{L}_{ILD} \downarrow	\mathcal{L}_{IPD} \downarrow
GAF-Net	0.86	0.22	3.86	0.75
w/o Gammatone	0.81	0.11	5.10	0.77
w/o GAFM	0.83	0.20	4.99	0.80
w/o DRG	0.85	0.31	4.61	1.00
Global DRG ^a	0.85	0.19	4.73	0.76

^a Global DRG generates a fixed gating factor g for each frequency.

4. RESULTS AND DISCUSSION

We evaluate the performance of the proposed GAF-Net and compare it with several baseline models [14, 15, 16, 17]. As shown in Table 1, GAF-Net performs well on key metrics that impact the binaural listening experience. The GAF-Net model’s strength lies in its accurate reconstruction of binaural intelligibility and spatial cues. GAF-Net achieves the highest average MBSTOI score, as well as the lowest average \mathcal{L}_{IPD} and \mathcal{L}_{ILD} , outperforming all baseline models. Furthermore, Δ PESQ result is suboptimal. Across speech quality metrics, the results reveal a profound trade-off. While large models like BCCTN demonstrate superior Δ PESQ, this often comes at the expense of higher spatial distortion and significant computational overhead. In contrast, GAF-Net maintains strong competitiveness on these metrics while also leading the way in binaural fidelity.

Furthermore, we found that GAF-Net achieves a remarkable balance between performance and efficiency, as shown in Table 2.

GAF-Net contains only 129.0 K parameters and 2.79 GMACs, with a computational cost of only 1.2% of larger models like BCCTN, yet surpasses them on key binaural performance metrics. Compared to LBCCN, GAF-Net achieves significant performance improvements with a slight increase in resources. Its real-time factor (RTF)¹ also meets the requirements of real-time applications. Therefore, GAF-Net stands out as a computationally efficient and high-performance solution, successfully bridging the performance and efficiency gap between existing methods.

The ablation study in Table 3 deconstructs the source of the GAF-Net model’s performance advantage. Removing features such as gammatone features or the GAFM backbone leads to an overall drop in performance, confirming the importance of dual-feature representation and global context modeling. Notably, analysis of DRG reveals a key trade-off: removing DRG improves Δ PESQ, but significantly worsens \mathcal{L}_{IPD} . This suggests that DRG intelligently trades off a degree of aggressive denoising in exchange for a significant reduction in spatial distortion and audible artifacts, which is crucial for a high-fidelity binaural listening experience.

5. CONCLUSION

This paper introduced GAF-Net, a lightweight deep complex network designed to address the performance-efficiency trade-off in binaural speech enhancement. With its innovative architecture, GAF-Net efficiently models global context while preserving spatial cues. With only 129 K parameters, it achieves STOA results on key metrics such as spatial completeness (\mathcal{L}_{IPD} and \mathcal{L}_{ILD}) and binaural clarity (MBSTOI). It also maintains strong competitiveness in speech quality compared to larger models. These findings validate GAF-Net as an efficient, low-resource solution for high-fidelity binaural audio applications. Future work will focus on evaluating its robustness in reverberant environments and extending its core components to other multichannel audio tasks.

¹The RTF is measured with Intel(R) Xeon(R) Gold 6146 CPU.

6. REFERENCES

- [1] Sharon Gannot, Emmanuel Vincent, Shmulik Markovich-Golan, and Alexey Ozerov, “A consolidated perspective on multimicrophone speech enhancement and source separation,” *IEEE/ACM Trans. Audio, Speech, Lang. Process.*, vol. 25, no. 4, pp. 692–730, 2017.
- [2] Chengshi Zheng, Huiyong Zhang, Wenzhe Liu, Xiaoxue Luo, Andong Li, Xiaodong Li, and Brian CJ Moore, “Sixty years of frequency-domain monaural speech enhancement: From traditional to deep learning methods,” *Trends Hear.*, vol. 27, pp. 23312165231209913, 2023.
- [3] Jens Blauert, *Spatial hearing: the psychophysics of human sound localization*, MIT press, 1997.
- [4] Xin Leng, Jingdong Chen, and Jacob Benesty, “On the compromise between noise reduction and speech/noise spatial information preservation in binaural speech enhancement,” *J. Acoust. Soc. Am.*, vol. 149, no. 5, pp. 3151–3162, 2021.
- [5] Vikas Tokala, Eric Grinstein, Mike Brookes, Simon Doclo, Jesper Jensen, and Patrick A Naylor, “Binaural speech enhancement using complex convolutional recurrent networks,” in *Proc. ACSSC*. IEEE, 2023, pp. 1130–1134.
- [6] Elior Hadad, Daniel Marquardt, Simon Doclo, and Sharon Gannot, “Theoretical analysis of binaural transfer function mvdr beamformers with interference cue preservation constraints,” *IEEE/ACM Trans. Audio, Speech, Lang. Process.*, vol. 23, no. 12, pp. 2449–2464, 2015.
- [7] Hala As’ad, Martin Bouchard, and Homayoun Kamkar-Parsi, “A robust target linearly constrained minimum variance beamformer with spatial cues preservation for binaural hearing aids,” *IEEE/ACM Trans. Audio, Speech, Lang. Process.*, vol. 27, no. 10, pp. 1549–1563, 2019.
- [8] Tim Van den Bogaert, Jan Wouters, Simon Doclo, and Marc Moonen, “Binaural cue preservation for hearing aids using an interaural transfer function multichannel wiener filter,” in *Proc. ICASSP*. IEEE, 2007, vol. 4, pp. IV–565.
- [9] Tim Van den Bogaert, Simon Doclo, Jan Wouters, and Marc Moonen, “Speech enhancement with multichannel wiener filter techniques in multimicrophone binaural hearing aids,” *J. Acoust. Soc. Am.*, vol. 125, no. 1, pp. 360–371, 2009.
- [10] Marvin Tammen and Simon Doclo, “Imposing correlation structures for deep binaural spatio-temporal wiener filtering,” *IEEE Trans. Audio, Speech, Lang. Process.*, vol. 33, pp. 1278–1292, 2025.
- [11] Chiheb Trabelsi, Olexa Bilaniuk, Ying Zhang, Dmitriy Serdyuk, Sandeep Subramanian, Joao Felipe Santos, Soroush Mehri, Negar Rostamzadeh, Yoshua Bengio, and Christopher J Pal, “Deep complex networks,” *arXiv preprint arXiv:1705.09792*, 2017.
- [12] Yanxin Hu, Yun Liu, Shubo Lv, Mengtao Xing, Shimin Zhang, Yihui Fu, Jian Wu, Bihong Zhang, and Lei Xie, “DCCRN: Deep complex convolution recurrent network for phase-aware speech enhancement,” *arXiv preprint arXiv:2008.00264*, 2020.
- [13] Vikas Tokala, Mike Brookes, and Patrick A Naylor, “Binaural speech enhancement using stoi-optimal masks,” in *Proc. IWAENC*. IEEE, 2022, pp. 1–5.
- [14] Xingwei Sun, Risheng Xia, Junfeng Li, and Yonghong Yan, “A deep learning based binaural speech enhancement approach with spatial cues preservation,” in *Proc. ICASSP*. IEEE, 2019, pp. 5766–5770.
- [15] Cong Han, Yi Luo, and Nima Mesgarani, “Real-time binaural speech separation with preserved spatial cues,” in *Proc. ICASSP*. IEEE, 2020, pp. 6404–6408.
- [16] Vikas Tokala, Eric Grinstein, Mike Brookes, Simon Doclo, Jesper Jensen, and Patrick A Naylor, “Binaural speech enhancement using deep complex convolutional transformer networks,” in *Proc. ICASSP*. IEEE, 2024, pp. 681–685.
- [17] Jingyuan Wang, Jie Zhang, Shihao Chen, and Miao Sun, “A lightweight and real-time binaural speech enhancement model with spatial cues preservation,” in *Proc. ICASSP*. IEEE, 2025, pp. 1–5.
- [18] Bosun Xie, *Head-related transfer function and virtual auditory display*, J. Ross Publishing, 2013.
- [19] Zicheng Feng, Yu Tsao, and Fei Chen, “Estimation and correction of relative transfer function for binaural speech separation networks to preserve spatial cues,” in *Proc. APSIPA ASC*. IEEE, 2021, pp. 1239–1244.
- [20] Zicheng Feng, Yu Tsao, and Fei Chen, “Recurrent neural network-based estimation and correction of relative transfer function for preserving spatial cues in speech separation,” in *Proc. EUSIPCO*. IEEE, 2022, pp. 155–159.
- [21] Junichi Yamagishi, Christophe Veaux, Kirsten MacDonald, et al., “CSTR VCTK Corpus: English multi-speaker corpus for CSTR voice cloning toolkit (version 0.92),” *University of Edinburgh. The Centre for Speech Technology Research (CSTR)*, pp. 271–350, 2019.
- [22] Fabian Brinkmann, Manoj Dinakaran, Robert Pelzer, Peter Grosche, Daniel Voss, and Stefan Weinzierl, “A cross-evaluated database of measured and simulated HRTFs including 3D head meshes, anthropometric features, and headphone impulse responses,” *J. Audio Eng. Soc.*, vol. 67, no. 9, pp. 705–718, 2019.
- [23] Andrew Varga and Herman JM Steeneken, “Assessment for automatic speech recognition: II. NOISEX-92: A database and an experiment to study the effect of additive noise on speech recognition systems,” *Speech Commun.*, vol. 12, no. 3, pp. 247–251, 1993.
- [24] Antony W Rix, John G Beerends, Michael P Hollier, and Andries P Hekstra, “Perceptual evaluation of speech quality (PESQ)-a new method for speech quality assessment of telephone networks and codecs,” in *Proc. ICASSP*. IEEE, 2001, vol. 2, pp. 749–752.
- [25] Asger Heidemann Andersen, Jan Mark de Haan, Zheng-Hua Tan, and Jesper Jensen, “Refinement and validation of the binaural short time objective intelligibility measure for spatially diverse conditions,” *Speech Commun.*, vol. 102, pp. 1–13, 2018.